The formation and differentiation of magmas

Bychkov D.A., Gnuchev Ya.Yu., Koptev-Dvornikov E.V. Calculation of saturated water contents in silicate melts in equilibrium with a pure water fluid *UDC 552.112*

M.V. Lomonosov Moscow State University, Department of Geology, Moscow (dmibychkov@gmail.com)

Abstract. Based on the experimental data extracted from the literature sources, a sample was formed containing the results of 394 hardening experiments characterizing the saturated water content in a wide range of intensive parameters of silicate systems.
An analysis of the main published types of models of water solubility in a silicate melt showed that the equation of Gordon Moore et al. best describes the experimental results.
The Moore equation recalibrated and converted to exponential form using an extended experimental sample allows, with an uncertainty not exceeding ±0.01 mole fraction, or ±0.2 wt. % to predict saturated water content in silicate melts in the ranges: melt compositions from basalts to rhyolites; pressure from atmospheric to 15 kbar; temperatures from 550 to 1300°C.

Keywords: water solubility equation, sample of water-saturated experiments, silicate melt.

Water is an incoherent component during the crystallization of rock-forming minerals of basic systems, accumulating in residual melts. When modeling the crystallization of water-containing systems, it is necessary to know the limit of water content in the melt, above which water forms an independent vapor phase. To do this, it is necessary to develop an equation that makes it possible to calculate the saturated concentration of water in the melt. Such an equation will also be useful for planning experiments with water-containing systems and testing the experimentally obtained water solubility in melts. Such an equation can be obtained either by choosing from previously proposed models of water solubility, or by developing an original equation.

To check the quality of the equations proposed so far that describe the saturated water content in silicate melts, it is necessary to form a sample of the corresponding experimental data. When analyzing the literature, 33 studies were found with the reduced content of dissolved water in a water-saturated melt, a total of 412 experiments.

The main data source for sampling was the INFOREX database (Ariskin et al., 1996). In addition to INFOREX, we used experimental data from works whose results were used to derive previously published equations (Shishkina et al., 2010; Berndt et al., 2002; Botcharnikov et al., 2004; Moore at al., 1995, 1998 ; Carrol and Blank., 1997; Silver et al., 1990; Shaw et al., 1963; Liu et al., 2005; Yamashita, 1999; Schmidt and Behrens, 2008).

The selection criteria for experiments in the sample were the availability of information on the equilibrium of a melt of known composition with a fluid phase containing no other components except water, temperature, and pressure.

After analyzing the main published types of water solubility equations in silicate melt (Almeev and Ariskin., 1996; Liu et al., 2005; Moore et al., 1998; Shishkina et al., 2010; Zhang et al., 2007), we came to concluded that the equation of Gordon Moore et al. best describes the experimental results.

In this equation, the dependence of the saturated water concentration on the composition of the melt is realized by taking into account the mole fractions of Al_2O_3, FeO, and Na_2O normalized to an anhydrous silicate matrix (Moore et al., 1998):

$$2\ln X_{\mathrm{H_2O}}^{melt} = \frac{a}{T} + \sum_{i=1}^{n} b_i X_i \left(\frac{P}{T}\right) + c\ln f_{\mathrm{H_2O}}^{fluid} + d, \quad (1)$$

where $X_{\mathrm{H_2O}}^{melt}$ is the saturated mole fraction of water in the melt; T is the temperature in degrees Kelvin; X_i is the mole fraction of oxide in the melt; P is the pressure in bars; $f_{\mathrm{H_2O}}^{fluid}$ – fluid water fugacity in bars, which was calculated using the modified Redlich-Kwong equation; a, b_i, c are the coefficients for the corresponding variables; d is a constant.

Since water fugacity is close to total pressure for a purely aqueous fluid, we decided to check how much the results of calculations of saturated water content using fugacity differ from the results using total pressure. It turned out that when using the same coefficients, the maximum difference between the results of calculations using these approaches does not exceed 0.08 wt % H_2O (for 41 experiments from Moore et al.). So, in order to simplify, we have reduced the Moore equation to the following form:

$$2\ln X_{\mathrm{H_2O}}^{melt} = \frac{a}{T} + \sum_{i=1}^{n} b_i X_i \left(\frac{P}{T}\right) + c\ln P + d, \quad (2)$$

From equation (2) follows the expression for the mole fraction of the saturated water content in the melt:

$$X_{\mathrm{H_2O}}^{melt} = \exp\left(\frac{a}{T} + \sum_{i=1}^{n} b_i X_i \left(\frac{P}{T}\right) + c\ln P + d\right) \quad (3)$$

where X_i are the mole fractions of the selected oxides in the single cationic form recalculated on an anhydrous basis. It should be noted that when transforming equation (2), the factor 2 was excluded.

Starting to recalibrate the equation of the form (3), we checked the optimality of the set of oxides proposed by Moore et al. The best results were achieved when the molar contents of FeO, CaO, $NaO_{0.5}$ were used as arguments. According to some literature data (Papale et al., 2006), the content of $KO_{0.5}$ in the melt has a noticeable effect on water solubility, however, testing of sets that included concentrations of $KO_{0.5}$ or the sum ($KO_{0.5}$ + $NaO_{0.5}$) led to an insignificant decrease in the sum squares of residues by 0.07%, despite the wide range of K_2O contents in our sample from 0 to 12.5 wt %, and the totals (K_2O + Na_2O) from 1.7 to 17.5 wt %.

When optimizing an equation of the form (3), experiments were removed for which the residuals exceeded 3σ, while the sample was reduced to 394 experiments. Polyhedron 394 of experimental compositions of melts in coordinates of oxide concentrations for the final sample is characterized by the following values (wt %): SiO_2 from 45.8 to 77.5, TiO_2 from 0 to 2.92, Al_2O_3 from 8 to 20.4, FeO* from 0.1 to 13.74 (FeO* – all iron converted to FeO), MgO from 0 to 9.59, CaO from 0 to 12.6, Na_2O from 1.2 to 9.72, K_2O from 0 to 12.25, P_2O_5 from 0 to 2.14. Thus, the sample contains compositions of melts from basalts to rhyolites.

The results of optimization of the equation with arguments in the form of molar concentrations of FeO, CaO, $NaO_{0.5}$ are shown in fig. 1a. The coefficients of this equation are shown in Table 1.

Table 1. Equation (3) parameters obtained as a result of data optimization on a sample of 394 experiments

a	b_{CaO}	b_{FeO}	$b_{NaO_{0.5}}$	c	d
440	-0.730	0.149	0.045	0.517	-5.55

An equation of the form (3) is preferably used for numerical modeling of magmatic evolution processes. At the same time, for many researchers who work directly with experimental or natural material, it is more convenient to calculate the solubility of water in mass percent, using as arguments the mass content of oxides in the melt, recalculated on an anhydrous basis:

$$C_{H_2O}^{melt} = \exp\left(\frac{a}{T} + \sum_{i=1}^{n} b_i C_i \left(\frac{P}{T}\right) + c \ln P + d\right) \qquad (4)$$

where C_i is the content of oxides in the melt, expressed in mass percent; $C_{H_2O}^{melt}$ - saturated water content in mass percent; see equations (1-3) for other designations.

The results of optimization of equation (4) with arguments in the form of mass percentages of FeO, CaO, Na_2O are shown in fig. 1b. The coefficients of this equation are shown in Table 2.

Table 2. Equation (4) parameters obtained as a result of data optimization on a sample of 394 experiments

a	b_{CaO}	b_{FeO}	$b_{NaO_{0.5}}$	c	d
447	-0.0094	0.0021	0.0050	0.628	-3.37

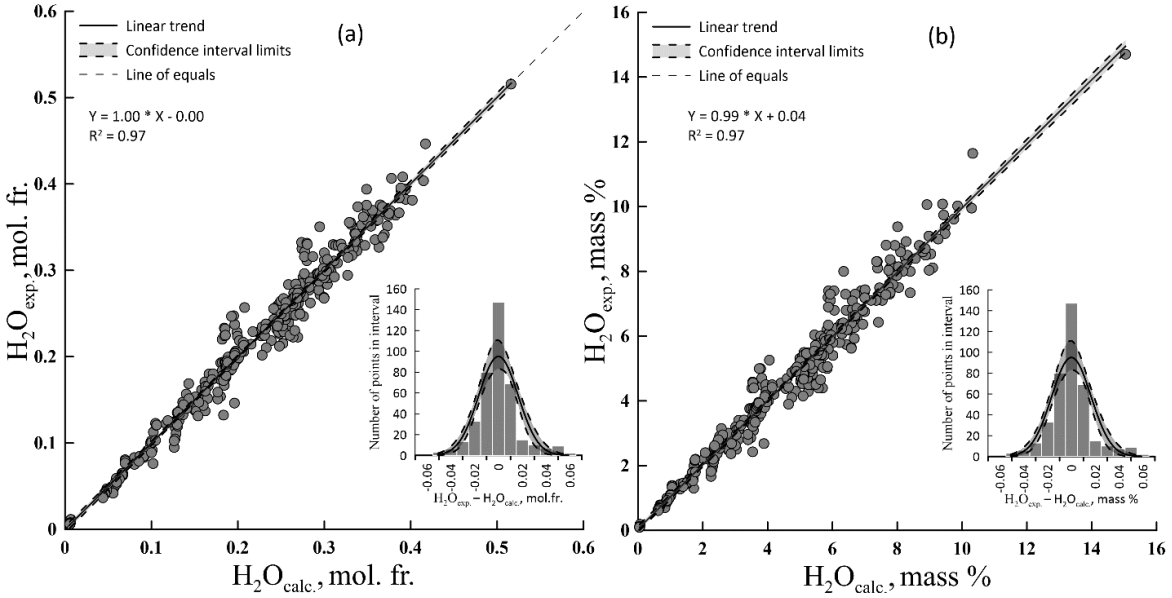

Fig. 1.: a - the result of optimizing the exponential equation of the form (3), b - the result of optimizing the exponential equation of the form (4); the dotted line is the confidence region at the 95% confidence level, 394 experiments in the sample.

Shown in fig. 1a and 1b, a comparison of the experimental and calculated data shows their good agreement, as evidenced by the closeness of the slope coefficients in the regression equations to unity, the free terms to zero, the values of the determination coefficients close to unity, and the very small width

of the confidence corridors. On fig. 1a, the maximum width of the confidence corridor in the region of high water contents does not exceed ±0.01 mole fraction (in the rest of the concentration range, it is much lower). On fig. 1b, the maximum width of the confidence corridor is ±0.2 wt. %. The nature of the histograms of the residuals in Figs. 1 demonstrates the proximity of distributions to normal and the unbiased estimates of water solubility. The calculated average deviations of the calculated concentrations from the experimental ones in mole fractions are – 0.000081, in mass percent – 0.0042. The standard deviations are 0.017 and 0.45, respectively, the range of deviations of the calculated values from the experimental values in mole fractions is from -0.051 to 0.059, in mass percent from -1.29 to 1.66%.

Thus, the optimization of the equations for calculating saturated water contents both in the form of mole fractions and in the form of mass percent showed close and very satisfactory results, despite the fact that the water contents in the experiments were determined by different methods: Fourier transform infrared spectroscopy (FTIR), secondary ion mass spectrometry (SIMS), tritium autoradiography, electron probe microanalysis (EPMA), Karl Fischer titration (KFT) and a number of other methods. A comparison of these methods, carried out in a number of works (Devine et al., 1995; Shishkina et al., 2010; Schmidt, Behrens, 2008; Silver et al., 1990, and many others), found that they all give consistent results, however, the EPMA method is characterized by the greatest dispersion, since its results are highly dependent on the quality of microprobe analysis, therefore, the authors of the reviews recommend that this method be selectively controlled by other more accurate, but also more labor-intensive methods. In the EPMA method, the water content is estimated from the difference between 100% and the sum of the oxide content determined by local microanalysis. Good agreement between different methods for determining the water content on the example of our initial sample (412 experiments) is shown in fig. 2.

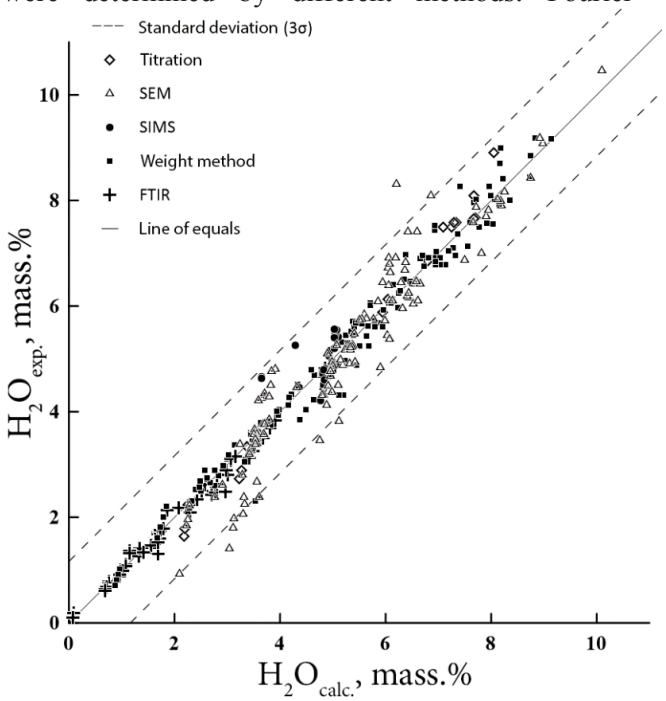

Fig. 2. Comparison of the experimental saturated water concentrations in the silicate melt determined by various methods with the results of calculating the water solubility according to equation (4) with the coefficients from Table 3. The dashed lines are the boundaries of the ±3σ corridor (412 experiments in the initial sample, 18 points were removed during optimization, outside the corridor).

Figure 2 clearly shows that the EPMA definitions are characterized by increased variance, however, most of them do not violate the general population of our sample.

Acknowledgments *The authors of the article are sincerely grateful to O.A. Lukanin, A.A. Borisov and N.S. Gorbachev for useful remarks that improved the quality of the study. We are especially grateful to the team led by A.A. Ariskin for providing the INFOREX database, which greatly simplified the search and evaluation of the necessary work.*

References:

Almeev, R. R., Ariskin, A. A. (1996) Mineral-melt equilibria in a hydrous basaltic system: computer modeling. Geochemistry International 34 (7), 563–573.

Ariskin A. A., Barmina G. S., Meshalkin S. S., Nikolaev G. S., Almeev R.R. (1996) INFOREX–3.0: A database on experimental studies of phase equilibria in igneous rocks and synthetic systems: II. Data description and petrological applications. Comput. Geosci. 22 (10) 1073–1082.

Berndt, J., Liebske., C., Holtz, F., Freise., M., Nowak, M., Ziegenbein., Hurkuck W., Koepke, J. (2002) A combined rapid-quench and H2-membrane setup for internally heated pressure vessels: Description and application for water solubility in basaltic melts. Am. Mineral. 87 (11–12), 1717–1726.

Botcharnikov, R. E., Koepke, J., Holtz, F., McCammon, C., Wilke, M. (2005) The effect of water activity on the oxidation and structural state of Fe in a ferro-basaltic melt. Geochim. Cosmochim. Acta. 69 (21), 5071–5085.

Carroll M. R., Blank J. G. (1997) The solubility of H_2O in phonolitic melts. Am. Mineral. 82 (5-6), 549–556.

Devine, J. D., Gardner, J. E., Brack, H. P., Layne, G. D., Rutherford, M. J. (1995) Comparison of microanalytical methods for estimating H_2O contents of silicic volcanic glasses. Am. Mineral. 80 (3–4), 319–328.

Liu, Y., Zhang, Y., Behrens, H. (2005) Solubility of H_2O in rhyolitic melts at low pressures and a new empirical model for mixed H_2O–CO_2 solubility in rhyolitic melts. J. Volcanol. Geotherm. Res., 143 (1–3), 219–235.

Moore G., Righter K., Carmichael I. S. E. (1995) The effect of dissolved water on the oxidation state of iron in natural silicate liquids. Contrib. Mineral. Petrol. 120 (2), 170–179.

Moore, G., Vennemann, T., Carmichael, I. S. E. (1998) An empirical model for the solubility of H2O in magmas to 3 kilobars. Am. Mineral. 83 (1–2), 36–42.

Papale, P., Moretti, R., Barbato, D. (2006) The compositional dependence of the saturation surface of H_2O+ CO_2 fluids in silicate melts. Chem. Geol. 229 (1–3), 78–95.

Schmidt, B. C., Behrens, H. (2008) Water solubility in phonolite melts: Influence of melt composition and temperature. Chem. Geol. 256 (3–4), 259–268.

Shaw, H. R. (1963) Obsidian-H_2O viscosities at 1000 and 2000 bars in the temperature range 700° to 900° C. J. Geophys. Res. 68 (23), 6337–6343.

Shishkina, T. A., Botcharnikov, R. E., Holtz, F., Almeev, R. R., Portnyagin, M. V. (2010) Solubility of H_2O-and CO_2-bearing fluids in tholeiitic basalts at pressures up to 500 MPa. Chem. Geol. 277 (1–2), 115–125.

Silver, L. A., Ihinger, P. D., Stolper, E. (1990) The influence of bulk composition on the speciation of water in silicate glasses. Contrib. Mineral. Petrol. 104 (2), 142–162.

Yamashita, S. (1999) Experimental study of the effect of temperature on water solubility in natural rhyolite melt to 100 MPa. J. Petrol. 40 (10), 1497–1507.

Zhang, Y., Xu, Z., Zhu, M., Wang, H. (2007) Silicate melt properties and volcanic eruptions. Rev. Geophys. 45 (4).

Bychkov D.A., Koptev-Dvornikov E.V. Comparison of simulation results of series of quenching experiments using cryminal and melts programs *UDC 550.41*

M.V. Lomonosov Moscow State University, Department of Geology, Moscow (dmibychkov@gmail.com)

Abstract. From the INFOREX database, 6 experimental series were selected, 3 of which represent the equilibrium crystallization of melts of the calc-alkaline series, and 3 of the tholeiitic series. The CriMinal program demonstrates a good reproduction of the experimental ratios of phases and compositions of melts and minerals for all six series considered. Comparison with calculations in the Melts program shows that our program simulates equilibrium at least as good for calc-alkaline compositions and noticeably better for tholeiitic ones.

Since the compositions of minerals are reproduced equally well by both programs, such a noticeable difference in the reproduction of the evolution of melt compositions is due to a distorted reproduction of the proportions of crystallization, which is especially noticeable from the moment the triple olivine-plagioclase-augite cotectic crystallization began. This result is consistent with the conclusion of A.A. Ariskin and G.S. Barmina that for correct numerical modeling of the crystallization of silicate systems, the correct calculation of the proportions of minerals crystallizing on cotectics is even more important than minimizing the error in estimating the phase composition.

Keywords: modeling, crystallization, silicate melt, equilibrium.

Material for verification of the CriMinal program (Bychkov, Koptev-Dvornikov, 2014) can be provided by experimental series of crystallization of a single initial composition with decreasing temperature.

Six experimental series were selected from the INFOREX database. On the common AFM diagram, three starting compositions fell into the area of tholeiite compositions, and three into the area of calc-alkaline compositions (Irvine and Baragar, 1971). As an example, we present the results of modeling the equilibrium crystallization of two of them (see Tables 1 and 2): one tholeiite (81) and one calc-alkaline (379).

Table 1. Experimental series presented to demonstrate the results of verification of the CriMinal program and a set of compositometers.

Publication number N*	Starting composition **	Experiment number in publication n***	Reference
81	BAS-1	1, 3-12, 15-20	(Thy, Lofgren, Imsland, 1991)
379	BAS-1	30-37	(Whitaker et al., 2007)

Notes. * Publication numbers (N) in the bibl.txt file of the INFOREX database. ** The name of the composition according to the INFOREX nomenclature. *** Experiment numbers (n) from each publication (N) in INFOREX database files.

Table 2. Starting compositions of the series used to demonstrate the results of verification of the CriMinal program and a set of compositometers.

Name	SiO_2	TiO_2	Al_2O_3	FeO	MnO	MgO	CaO	Na_2O	K_2O	P_2O_5
81 BAS-1	46.8	2.32	13.75	10.15	0.18	9.9	11.12	2.62	1.47	0.49
379 BAS-1	47.53	1.43	15.03	10.53	0.16	10.46	10.57	2.18	0.42	0.26

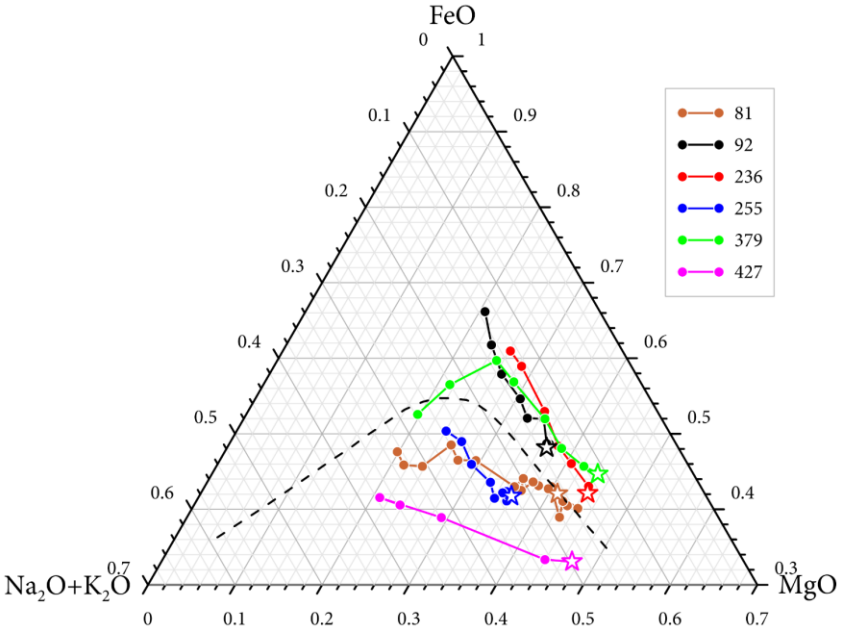

Fig. 1. Position of starting compositions and experimental points of melt evolution on the AFM diagram. The numbers in the legend correspond to the numbers of publications in the INFOREX database. Asterisks indicate the respective starting lineups. The dotted line is the boundary between the fields of tholeiitic and calc-alkaline compositions (Irvine and Baragar, 1971).

A comparison of the experimental and predicted phase compositions and compositions of melts by CriMinal is presented in a series of figures 2 through 5. For comparison, the same figures show the results of modeling the equilibrium crystallization of the same initial compositions using the currently popular Melts program.

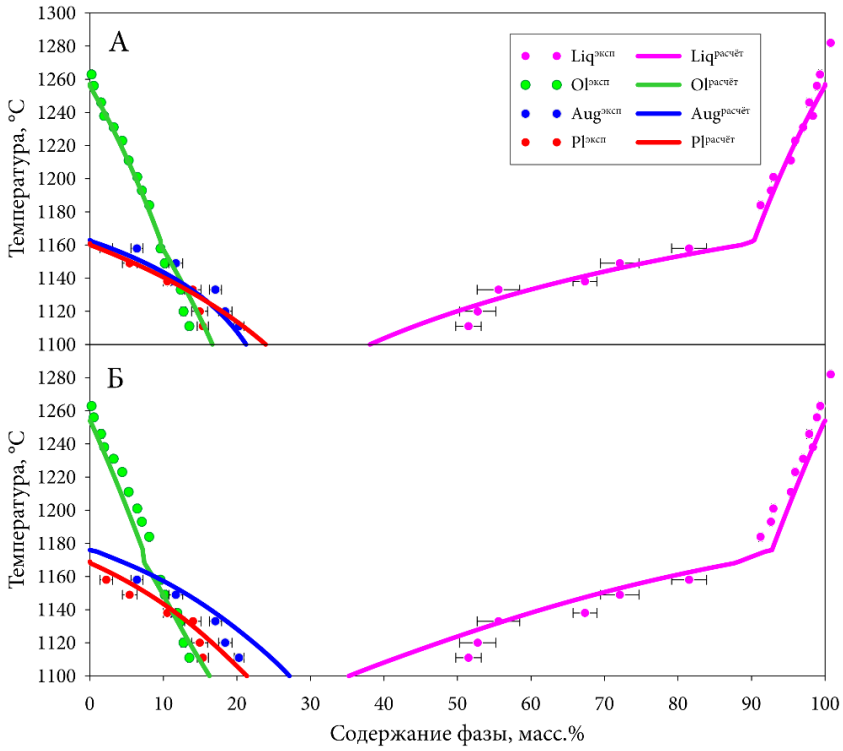

Fig. 2. Graph of the change in the phase composition of the system during equilibrium crystallization of the 81 BAS-1 basalt composition. Points – mass balance recalculation of experimental data; lines: A - the result of the calculation of CriMinal; B is the result of Melts calculation.

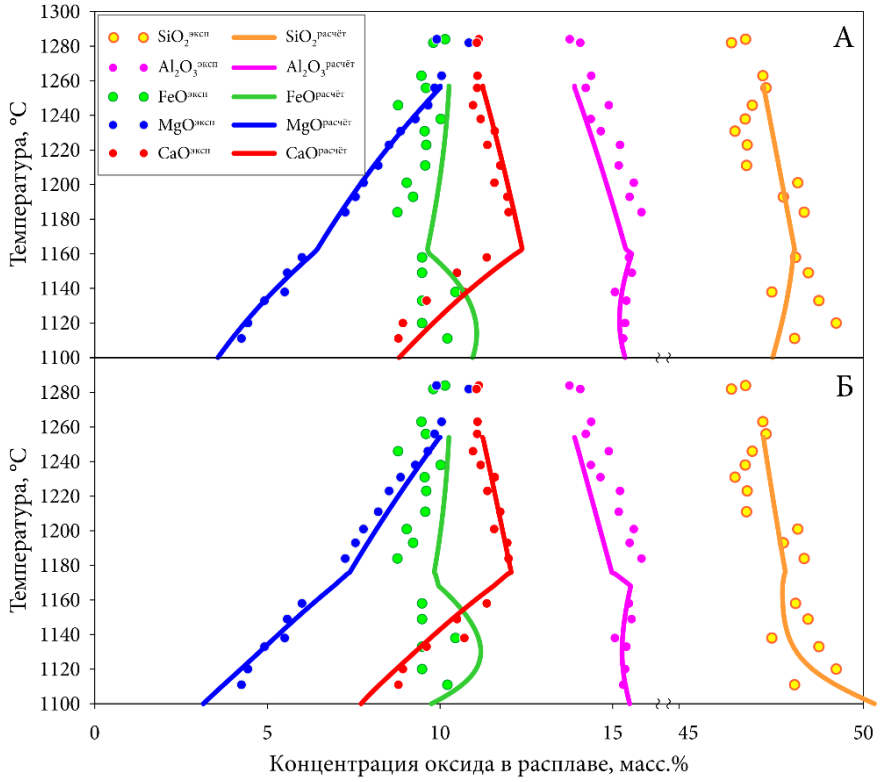

Fig. 3. Graph of changes in the content of melt macrocomponents during equilibrium crystallization of 81 BAS-1 basalt composition. Dots are the result of glass analysis; lines: A - the result of the calculation of CriMinal; B is the result of Melts calculation.

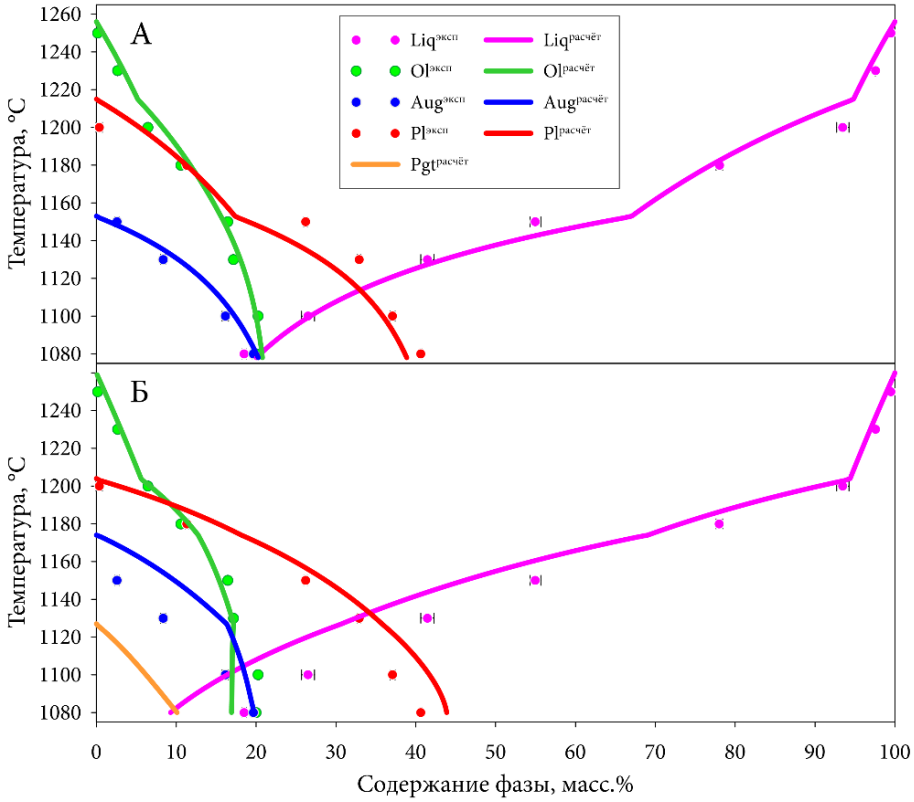

Fig. 4. Graph of changes in the phase composition of the system during equilibrium crystallization of basalt composition 379 BAS-1. Points – mass balance recalculation of experimental data; lines: A - the result of the calculation of CriMinal; B is the result of Melts calculation.

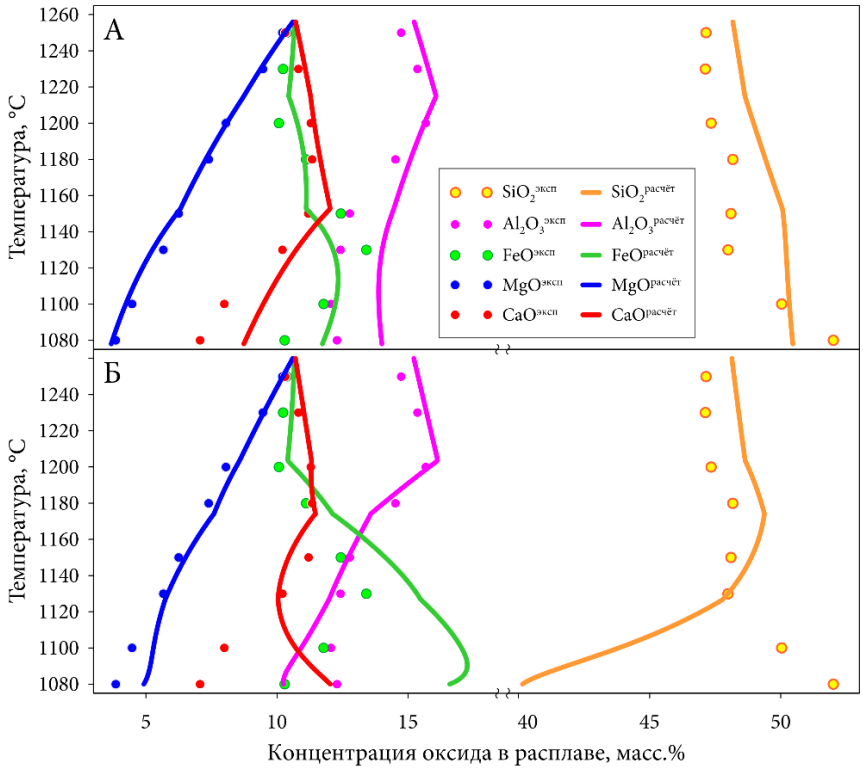

Fig. 5. Graph of changes in the content of melt macrocomponents during equilibrium crystallization of basalt composition 379 BAS-1. Dots are the result of glass analysis; lines: A - the result of the calculation of CriMinal; B is the result of Melts calculation.

Calculations in the CriMinal program demonstrate good reproduction of the experimental ratios of phases and compositions of melts and minerals for all six series considered. Comparison with calculations using the Melts program shows that our program simulates equilibrium at least as good for calc-alkaline compositions and noticeably better for tholeiitic ones.

Acknowledgments *We are especially grateful to the team led by A.A. Ariskin for providing the INFOREX database, which greatly simplified the search and evaluation of the necessary work.*

References:

1. Bychkov D., Koptev-Dvornikov E. The Software for Simulation of Equilibrium Crystallization // Goldschmidt2014 Abstracts. : http://goldschmidt.info/2014/uploads/abstracts/finalPDFs/A-Z.pdf, 2014. С. 319–319.
2. Irvine T. N., Baragar W. R. A. A guide to the chemical classification of the common volcanic rocks // Canadian Journal of Earth Sciences. 1971. Т. 8. № 5. С. 523–548.
3. Thy P., Lofgren G. E. Experimental constraints on the low-pressure evolution of transitional and mildly alkalic basalts: multisaturated liquids and coexisting augites // Contr. Mineral. and Petrol. 1992. Т. 112. № 2–3. С. 196–202.
4. Whitaker M. L. et al.. The Role of Pressure in Producing Compositional Diversity in Intraplate Basaltic Magmas // Journal of Petrology. 2007. Т. 48. № 2. С. 365–393.

Chevychelov* V.Y., Viryus A.A., Kotelnikov A. R., Suk N.I. Formation of carbonate-alkaline and carbonate-silicate melts as a result of low-pressure and high-temperature melting of marly limestone *UDC 550.42; UDC 550.42*

D.S. Korzhinskii Institute of Experimental Mineralogy of Russian Academy of Sciences (IEM RAS); chev@iem.ac.ru*, allavirus@yandex.ru, kotelnik1950@yandex.ru, sukni@iem.ac.ru

Abstract. The experiments were carried out at T=1300 (1250)°C, P=7 -17 MPa and elevated CO_2 partial pressure. Our task was to determine the conditions for the formation of carbonate-silicate rocks formed as a result of the melting of limestone containing 40 wt.% pelitic material (from the Khamaryn-Khural-Khiid combustion metamorphic complex, East Mongolia). The mineral composition of the sample used in the experiments is as follows: calcite (~59.5 wt.%), aggregates of melilite + clinopyroxene + nepheline; quartz, albite-anorthoclase, plagioclase, zircon, etc. are less common. The main phases in the solid products of the experiments are larnite, gelenite (?), and calcite, but in addition to them, four more carbonate-containing phases were found: the products of quenching of a carbonate-alkaline melt and three varieties of quenched carbonate-silicate glasses. The physicochemical

conditions for the synthesis and stability of these phases may be of interest from the point of view of the possibility of their formation under natural conditions. Semi-quantitative assessment of the carbon content in Si-Al varieties of carbonate-silicate glass was performed using the microprobe analysis (EPMA).

Keywords: melting of marly limestone; carbonate-alkaline melt; carbonate-silicate melts; experiment

The results of low-pressure and high-temperature experiments on the melting of marly limestone from the Khamaryn-Khural-Khiid combustion metamorphic complex at a relatively high temperature, low pressure, and elevated partial pressure of CO_2 are presented. Such complexes in Mongolia were formed at high-temperature metamorphism and partial melting of carbonate-silicate sedimentary rocks caused by natural underground coal fires (Savina et al., 2020; Peretyazhko et al., 2021; Kalugin et al., 2005). The task of our experimental studies was to determine the conditions for the formation of carbonate-silicate rocks formed as a result of incongruent melting of limestone containing about 40 wt.% pelitic material.

The chemical composition of the carbonate-silicate rock of MN-1423 used in the experiments (wt. %): 16.3 SiO_2, 0.3 TiO_2, 9.1 Al_2O_3, 0.8 Fe_2O_3, 0.4 FeO, 0.1 MnO, 1.9 MgO, 39.9 CaO, 2.6 Na_2O, 0.3 K_2O, 0.2 P_2O_5, 26.2 CO_2, 1.5 H_2O^+, 0.5 H_2O^-, 0.2 S_{tot}, 0.2 SrO, 100.6 Σ. The mineral composition of this sample is as follows: calcite (~59.5 wt. %), melilite + clinopyroxene + nepheline aggregates, less common quartz, albite-anorthoclase, plagioclase, zircon, etc. (Peretyazhko et al., 2021).

The experiments were carried out in platinum capsules. Most of the experiments were carried out in two stages. "Internally heated pressure vessel" (IHPV, gas bomb) at the IEM RAS was used for the experiments. The oxygen fugacity f_{O2} inside the capsule corresponded to approximately (Ni-NiO) + 3.5, according to the estimate given in (Berndt et al., 2005).

A powder of the carbonate-silicate rock under study (20–50 mg) was placed in one small capsule (4 mm × 0.2 mm × 18–20 mm), and a freshly prepared silver oxalate $Ag_2C_2O_4$ (30–40 mg) was placed in other small capsule. The silver oxalate was synthesized according to reactions $2AgNO_3 + Na_2C_2O_4 \rightarrow Ag_2C_2O_4\downarrow + 2NaNO_3$ by pouring together two salt solutions and drying the repeatedly washed precipitate. After that, the capsules were squeezed 2/3 of their length, but were not welded shut, and placed inside a large capsule (10 mm × 0.2 mm × 50 mm), which then was welded shut. At the first low-temperature stage of the experiment, the structure of three capsules assembled in this way was kept at 120-130°C in the oven for 2-4 hours to decompose silver oxalate by the reaction $Ag_2C_2O_4 \rightarrow 2Ag + 2CO_2\uparrow$. The second high-temperature stage was carried out in the IHPV at T =1300 (1250)°C, P =7 -17 MPa. Its duration was 5.5-6.5 hours.

After the experiment, a large capsule was "inflated" due to the excess gas phase inside. The experiment was opened up as follows: (1) the capsule was weighed, (2) the capsule was frozen in liquid nitrogen for 3 min., (3) the capsule was taken out of the Dewar vessel with liquid nitrogen, several holes were pierced in it and kept for 3 min in air for heating to room temperature, while the excess gas phase (CO_2) was removed from the capsule through the holes, (4) the capsule was weighed, (5) the capsule was heated at 100°C in an oven for 3 min., while the liquid phase (H_2O) was removed from the capsule through the holes, (6) then the capsule was kept in air for 3 min to cool to room temperature and weighed. After the experiments, the solid products were analyzed by X-ray spectral electron probe analysis (EPMA) using energy-dispersive and wave X-ray spectrometers. The semi-quantitative assessment of the carbon content in the glasses was also carried out by the EPMA method.

Table 1. Experimental conditions and results

Num-ber run	Initial composition of the run	First stage of the run [1]			Second stage of the run			After the run		
		T°, C	P_{total}, MPa	Durati-on, hour	T°, C	P_{total}, MPa	Durati-on, hour	Weight of gas/ liquid phases in an capsule, mg	Decom-posed calcite in the charge, mg	Preser-ved calcite in the charge, mg/wt.%
PRT-1a	Charge (50.2 mg)	-	-	-	~1300	~9.7-9.9	~5.9	10.7/0.1	24.4	5.5/18.3
PRT-1b	Charge (50.5 mg); H_2O (5.4 mg)	-	-	-	~1300	~9.7-9.9	~5.9	10.5/5.0	23.9	6.2/20.6
PRT-1c [2]	Charge (50.4 mg); $H_2C_2O_4 \times 2H_2$	-	-	-	~1300	~9.8-9.9	~5.75	-	-	-

Number run	Initial composition of the run	First stage of the run [1]			Second stage of the run			After the run		
		T^o, C	P_{total}, MPa	Duration, hour	T^o, C	P_{total}, MPa	Duration, hour	Weight of gas/ liquid phases in an capsule, mg	Decomposed calcite in the charge, mg	Preserved calcite in the charge, mg/wt.%
	O (24.7 mg)									
PRT-2a	Charge (49.2 mg); $Ag_2C_2O_4$ (30.8 mg)	150-160	~4.2-4.4	~0.9	~1300	~7.0-9.7	~5.4	18.7/0.7	22.2	7.0/24.0
PRT-2b	Charge (20.4 mg); $Ag_2C_2O_4$ (39.7 mg)	115-160	~7.6-7.9	~1.4	~1300	~12.1-12.5	~5.8	15.5/0.5	9.1	3.0/25.2
PRT-3	Charge (55.9 mg); $Ag_2C_2O_4$ (50.7 mg)	130-140 140-180	<3-5 ~4.0-4.6	4.5 ~1.9	~1300	~6.9-6.8	~6.5	26.5/1.0	27.0	6.3/18.9
PRT-4	Charge (21.3 mg); $Ag_2C_2O_4$ (42.1 mg)	~130	<3-5	~3.3	~1250	~17.3-17.4	~6.1	16.6/1.1	9.9	2.8/22.0

[1] In the experiments PRT-1a, PRT-1b and PRT-1c, the first stage was absent.
[2] This experiment was opened up without determining the contents of the gas and liquid phases inside the capsule.

The weight of the gas phase released from the capsule upon opening varied from 10.5 to ~26.5 mg depending on the weight of the initial charge and silver oxalate. The excess gas phase was represented by CO_2. Partially, the gas phase was formed during the first low-temperature stage of the experiment due to the decomposition of silver oxalate, and the rest at the second high-temperature stage due to the decomposition of calcite from the studied carbonate-silicate rock. The weight of the liquid phase released from the capsule (practically one H_2O), as expected, was extremely small, from 0.1 to 1.1 mg, and only in the PRT-1b experiment containing ~5.4 mg of initial H_2O, ~5 mg of liquid was released upon opening.

Knowing the weights of the gas (m_g) and liquid (m_l) phases released from the capsule upon opening each experiment, we can estimate the possible amount of both decomposed ($Cal_{decomposed}$) and preserved (Cal) calcite in the charge after the experiment. The calculation was carried out as follows. The content of calcite in the original charge is approximately 59.47 wt.%, based on the fact that the content of CO_2 in the charge is 26.15 wt.%, and calcite ($CaCO_3$) contains 43.97 wt.% CO_2. Knowing the mass of the charge (m_{charge}) in each experiment, we can calculate the mass of the initial calcite ($m_{charge} \times 0.5947$). For experiments with initial silver oxalate, the amount of CO_2 released at the complete decomposition of oxalate can be calculated ($m_{Ag2C2O4} \times 0.29$). Then the possible amount of decomposed calcite is calculated by the formula $Cal_{decomposed} = (m_g - (m_{Ag2C2O4} \times 0.29)) : 0.4397$, and the amount of calcite remaining in the charge is calculated by the following formula $Cal = (m_{charge} \times 0.5947) - Cal_{decomposed}$. In experiments of PRT-1a and PRT-1b, which did not contain the initial silver oxalate, the entire gas phase released from the capsule was formed at the decomposition of calcite of the charge.

In all six experiments carried out at different conditions, approximately the same amount of undecomposed calcite in the charge was obtained ~18 -25 wt.%. This shows that the technique we used to preliminarily create an elevated CO_2 pressure in the capsule due to the decomposition of silver oxalate, unfortunately, does not prevent the decomposition of calcite in the charge at the experimental parameters and most of the initial calcite (~75-82 wt.%) decomposes during the experiment.

Table 2. Chemical compositions of the solid phases obtained in the experiments (EPMA method, oxides of elements, wt. %)

Item №	Phase	n [1]	SiO_2	TiO_2	Al_2O_3	MgO	CaO	SrO	Na_2O	K_2O	SO_3	Σ
1	Larnite, Ca_2SiO_4	39	28.2 ±3.1	-	0.5 ±0.5	1.1 ±0.9	65.5 ±2.2	-	2.0 ±0.7	-	-	99.0 ±3.9
2	Gelenite (?), $Ca_2Al_2SiO_7$	37	12.0 ±7.3	-	39.0 ±7.4	1.3 ±1.6	46.2 ±4.1	-	0.6 ±0.5	-	-	100.6 ±3.1
3	Calcite [2], $Ca(CO_3)$	18	-	-	-	-	57.0 ±2.4	0.7 ±0.5	-	-	-	59.5 ±2.5
4	Quenched products of carbonate-alkaline melt [2]	31	-	-	-	-	33.9 ±4.0	-	12.8 ±3.0	4.3 ±1.0	3.3 ±2.6	57.2 ±4.4
5_{total}	Quenched carbonate-silicate glass [2]	23	15.4 ±9.6	0.5 ±0.4	10.2 ±7.7	2.3 ±1.6	43.8 ±4.9	-	3.0 ±2.2	0.5 ±0.3	-	77.5 ±7.4
5_a	Quenched carbonate-silicate (Si-Al) glass [2]	8	14.3 ±0.5	0.7 ±0.4	10.0 ±0.5	2.5 ±0.5	46.5 ±1.8	-	3.0 ±0.5	0.4 ±0.2	-	79.2 ±2.9
5_b	Quenched carbonate-silicate (Si) glass [2]	6	29.1 ±5.5	-	1.1 ±1.1	0.5 ±0.3	45.1 ±5.4	-	1.9 ±0.5	0.4 ±0.2	-	80.0 ±3.5
5_c	Quenched carbonate-silicate (Mg-Si) glass [2]	5	4.8 ±1.0	-	1.4 ±0.5	10.8 ±0.8	51.8 ±0.9	-	1.3 ±0.5	-	(0-1.3) ±0.5	72.4 ±1.5
6	Periclase, (Mg,Al)O	1	1.0 ±0.5	1.3 ±0.4	10.9 ±1.0	74.9 ±1.6	2.6 ±0.4	-	-	-	-	92.7 ±4.0
7	Magnesium aluminate, $Mg(AlO_2)_2$	3	2.1 ±0.6	-	67.0 ±2.8	26.3 ±1.0	1.7 ±1.0	-	0.4 ±0.4	-	-	99.8 ±2.1
8	Phase $CaTiSiO_5$ (?)	12	15.1 ±8.2	25.2 ±10.9	3.9 ±2.5	3.7 ±2.5	50.3 ±3.3	-	1.0 ±0.4	-	-	103.1 ±4.1

[1] – n - number of performed analyses of this phase. [2] - Phase contains $CO_2(CO_3^{2-})$.

The solid products of the experiments are represented by the phases listed in Table 2, as well as CaS sulfide. Among these phases, in addition to preserved calcite, there are four carbonate-containing phases (quenched products of carbonate-alkaline melt (4) and three types of quenched carbonate-silicate glasses (5a, 5b, 5c)), stable at *P-T* parameters of the experiments. The physicochemical conditions of the synthesis and stability of these phases may be of interest from the point of view of the possibility of their formation at natural conditions. The obtained experimental results show different conditions for the formation of these phases. So, the quenched products of carbonate-alkaline melt were found in all experiments, and quenched carbonate-silicate glasses were obtained only in experiments containing silver oxalate, due to the decomposition of which, an increased CO_2 pressure was created at the first stage

of experiments at a relatively low temperature. Moreover, if (5a) carbonate-silicate (Si-Al) melt is stable at P_{total} ~12.1-12.5 MPa and T ~1300°C, then (5b) carbonate-silicate (Si) melt was obtained at P_{total} ~17.3-17.4 MPa and T ~1250°C, and (5c) carbonate-silicate (Mg-Si) melt was synthesized at P_{total} ~6.8-12.5 MPa and T ~1300°C.

Quenched carbonate-silicate (Si-Al) glass (5a) was investigated by us in more detail. The aim of the study was to evaluate (semi-quantitative determination) the content of (CO_3^{2-}) in the glass composition. Since glass is not a conductor, the samples were sprayed with carbon. To take into account the intensity of carbon emitted by the carbon-spray film, the content of carbon was determined not only in glass, but also in carbon-free quartz and in stoichiometric calcite. Glass, calcite, and quartz were placed in one block, sprayed with a thin layer of carbon of the same thickness. The carbon content in quartz was about 10 wt. % or about 35 wt. % in terms of CO_2. We believe that carbon film gives such a carbon content. The oxygen content was calculated from the stoichiometry of the composition, attributing oxygen to both carbon and silicon. Therefore, the proportion of excess carbon content in quartz was calculated from the weight contents of oxides (CO_2/SiO_2).

Based on the assumption that the glass at study contains carbon in the form of carbon oxide (CO_3^{2-}), it was convenient to use stoichiometric calcite sprayed with carbon of the same thickness as the glass as the main standard for the estimated semi-quantitative determination of carbon content. The carbon content in calcite turned out to be overestimated by 3-4 wt. %, and in terms of CO_2 by 12 -17 wt. %. In all cases, the proportion of excess carbon in the total carbon content averaged ~25–26 wt. %.

Thus, the approximate carbon content in the glass at study can be calculated taking into account the proportion of excess (extra) carbon found from calcite and amounting to ~25-26 wt. % according to the formula: $m(C) = m(C_i) - m(C_i)*0.26$, where $m(C_i)$ is the measured carbon content in glass, and 0.26 is the proportion of excess (extra) carbon content.

The results of this calculation show that the content of carbon oxide in the carbonate-silicate (Si-Al) glass (5a) is ~18.4 wt. % (wave spectrometer, average over three measurements) and ~18.7 wt. % (energy-dispersive spectrometer, average over six measurements), which is close to ~20.8 wt. %, determined from the deficit of the total amount (Table 2).

Funding. *This study was carried out under government-financed research project of IEM RAS No. FMUF-2022-0004 and FMUF-2022-0003.*

References

Kalugin V.M., Maksimova N.V., Nigmatulina E.N., Sokol E.V., Sharygin V.V. Combustion metamorphism. Moscow: SO RAN. 2005. 307 p. (in Russian).

Savina E.A., Peretyazhko I.S., Khromova E.A., Glushkova V.E. Melted Rocks (Clinkers and Paralavas) of Khamaryn-Khural-Khiid Combustion Metamorphic Complex in Eastern Mongolia: Mineralogy, Geochemistry and Formation Processes // Petrology. 2020. V. 28. № 5. P. 431-457.

Berndt J., Koepke J., Holtz Fr. An experimental investigation of the influence of water and oxygen fugacity on differentiation of MORB at 200 MPa // J. Petrol. 2005. V. 46. № 1. P. 135–167.

Peretyazhko I.S., Savina E.A., Khromova E.A Low-pressure (> 4 MPa) and high-temperature (> 1250°C) incongruent melting of marly limestone: formation of carbonate melt and melilite-nepheline paralava in the Khramaryn-Khural-Khiid combustion metamorphic complex, East Mongolia // Contributions to Mineralogy and Petrology. 2021. V. 176. No 5. p. 38.